 Human Molecular Genetics, 1997, Vol. 6, No. 11 **1771–1780**

ARTICLE

Frataxin is reduced in Friedreich ataxia patients and is associated with mitochondrial membranes

Victoria Campuzano, Laura Montermini[1], Yves Lutz, Lidia Cova[1,2], Colette Hindelang, Sarn Jiralerspong[1], Yvon Trottier, Stephen J. Kish[3], Baptiste Faucheux[4], Paul Trouillas[5], François J. Authier[6], Alexandra Dürr[4], Jean-Louis Mandel, Angelo Vescovi[2], Massimo Pandolfo[1,7,8] and Michel Koenig*

Institut de Génétique et de Biologie Moléculaire et Cellulaire, INSERM-CNRS-ULP, Illkirch, France, [1]Centre de Recherche du CHUM, Pavillon Notre Dame, Montréal, Canada, [2]Laboratory of Neuropharmacology, Istituto Nazionale Neurologico 'C.Besta', Milan, Italy, [3]Clarke Institute of Psychiatry, Toronto, Canada, [4]Hôpital Pitié-Salpêtrière, Paris, France, [5]Hôpital Neurologique et Neuro-Chirurgical Pierre Wertheimer, Lyon, France, [6]Hôpital Henri Mondor, Creteil, France, [7]Département de Médecine, Université de Montréal, Montréal, Canada and [8]Department of Neurology and Neurosurgery, McGill University, Montréal, Canada

Received April 29, 1997; Revised and Accepted July 23, 1997

Friedreich ataxia is a progressive neurodegenerative disorder caused by loss of function mutations in the frataxin gene. In order to unravel frataxin function we developed monoclonal antibodies raised against different regions of the protein. These antibodies detect a processed 18 kDa protein in various human and mouse tissues and cell lines that is severely reduced in Friedreich ataxia patients. By immunocytofluorescence and immunocytoelectron microscopy we show that frataxin is located in mitochondria, associated with the mitochondrial membranes and crests. Analysis of cellular localization of various truncated forms of frataxin expressed in cultured cells and evidence of removal of an N-terminal epitope during protein maturation demonstrated that the mitochondrial targetting sequence is encoded by the first 20 amino acids. Given the shared clinical features between Friedreich ataxia, vitamin E deficiency and some mitochondriopathies, our data suggest that a reduction in frataxin results in oxidative damage.

INTRODUCTION

Progressive neurodegenerative diseases are conditions that unrelentingly lead to severe physical disability or death. Neurons with long myelinated axons running through the spinal cord are affected by many of these diseases. These neurons may be considered giant cells, which must bear a heavy burden for cell maintenance and the underlying energy needs. The largest neurons in the human body are those located in the dorsal root ganglia of the spinal cord. The corresponding axons, that may be more than 1 m long, run from the peripheral sensory endings through the sensory nerves and the posterior columns of the spinal cord, up to the medulla oblongata. These neurons are primarily affected in Friedreich ataxia (FRDA), an autosomal recessive progressive neurodegenerative disorder which is the most common cause of inherited ataxia in the Caucasian population (1). Other sites of neurodegeneration in Friedreich ataxia involve neurons of the spinocerebellar and corticospinal tracts (2). Non-neuronal lesions are also found in Friedreich ataxia, including hypertrophic cardiomyopathy present in most patients. Diabetes or glucose intolerance are common and possibly relate to pancreatic deficiency. All the involved tissues are highly sensitive to impaired energy production, as evidenced by their frequent involvement in mitochondrial diseases (3).

Friedreich ataxia is most commonly caused by a large GAA triplet repeat expansion within the first intron of the gene encoding frataxin (4). The majority of patients (~95%) are homozygous for the GAA repeat expansion and the remaining 5% are compound heterozygous for the expansion and a point mutation affecting the frataxin coding sequence. In patients homozygous for the expansion there is a correlation between the number of GAA repeats on the smaller allele and age of onset, disease progression and cardiomyopathy (5–9), confirming that the expansion is the primary cause of the disease. The expansion causes severely reduced levels of mature frataxin mRNA (4,10). The existence of nonsense and splice mutations leading to the

*To whom correspondence should be addressed. Tel: +33 3 8865 3399; Fax: +33 3 8865 3246; Email: mkoenig@igbmc.u-strasbg.fr

same clinical presentation as homozygous expansions and the reduced levels of frataxin mRNA found associated with homozygous expansions indicate that Friedreich ataxia is due to loss of frataxin function.

Frataxin is a predicted 210 amino acid protein with no homology with proteins of known function. Related genes have been found in the mouse (11) and, as anonymous open reading frames (ORFs), in the nematode *Caenorhabditis elegans* and in yeast (4). Frataxin also shows low but significant similarity with the CyaY proteins of Gram-negative bacteria, whose function is unknown (12). The domain encoded by human exons 3–5 shows the highest conservation throughout evolution.

In order to unravel how frataxin loss of function causes the disease, we sought to identify frataxin in cells of normal and affected individuals. We developed specific monoclonal antibodies (mAbs) raised against different regions of the protein. These mAbs detect an 18 kDa protein that is severely reduced in tissues of FRDA patients. An inverse correlation was observed between the amount of protein and expansion size on the smaller allele. Using immunofluorescence and immunoelectron microscopy we show that frataxin localizes within the mitochondria and we found that the mitochondrial target sequence is encoded by exon 1 of the frataxin gene.

RESULTS

Antibody production and characterization

In order to develop mAbs against frataxin the complete coding sequence of human frataxin was cloned in the prokaryotic expression vector pATH (13). Overexpression of pATH constructs in *Escherichia coli* produced fusion proteins (containing the TrpE bacterial protein at the N-terminal end) as inclusion bodies, which were isolated and injected into mice to generate antibodies. Peptide A, a potentially immunogenic peptide from the N-terminus (Fig. 1A), was also injected into mice for mAb production. Mice sera and supernatants of positive hybridoma clones were tested by Western blot of transfected COS-1 cells overexpressing the full-length frataxin protein. Five specific hybridomas were established, 1D4, 2D4, 2F10 and 1G2 raised against the fusion protein and 1H1 raised against N-terminal peptide A. Under our experimental conditions endogenous frataxin was undetectable in non-transfected COS-1 cells. On Western blots of transfected COS-1 cells all mAbs detected an ~30 kDa protein and smaller products that showed intensity pattern variations, depending on the antibody used (Fig. 1B). The full-length 30 kDa frataxin expressed in COS-1 cells was identical in size to the *in vitro* translated protein (data not shown), excluding the possibility of major post-translational modification.

In order to map the region of frataxin recognized by each anti-fusion protein mAb we expressed different forms of frataxin truncated at the C-terminus in COS-1 cells. Western blot analysis of these constructs indicated that antibodies 1D4, 2F10 and 1G2 recognize epitopes encoded by exon 4, while antibody 2D4 recognizes an epitope encoded by exon 1 or 2 (Fig. 1B), as does anti-peptide A antibody 1H1. An ELISA test with synthetic polypeptides showed that mAbs 1H1 and 2D4 both recognize peptide A (not shown). Antibodies 1D4, 2F10 and 1G2 do not cross-react with overlapping peptides that encompass exon 4 and flanking encoded sequences, suggesting that they recognize

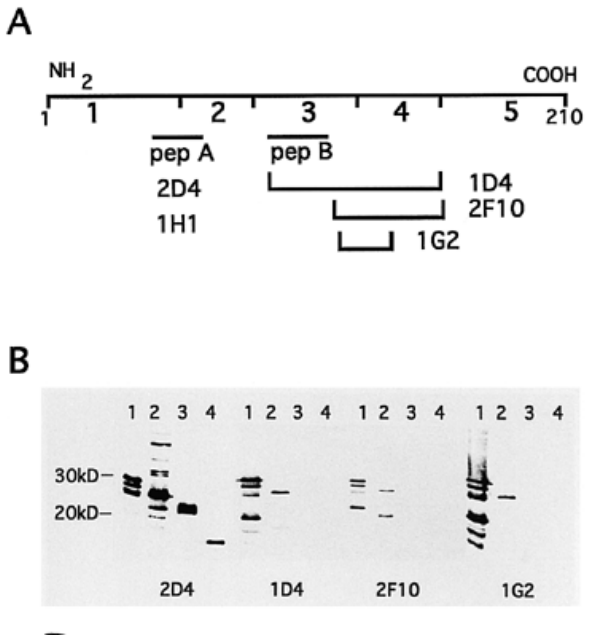

Figure 1. Epitope mapping of frataxin antibodies. (**A**) Localization of the epitopes recognized by the different antibodies with respect to the exon boundaries, peptides A (CGLRTDIDATCTPRRASSNQRG) and B (ERLAEETLDSLAEFFEDLADK) and the G130V mutation. (**B**) Different forms of frataxin truncated at the C-terminus were overexpressed in COS-1 cells and analysed by Western blot. Lane 1, full-length protein (exons 1–5); lane 2, exons 1–4 (amino acids 1–161); lane 3, exons 1–3 (amino acids 1–128); lane 4, exons 1–2 (amino acids 1–88). Antibodies 1D4, 2F10 and 1G2 recognize only the forms including exon 4 (lanes 1 and 2), while antibody 2D4 detects an epitope coded by exon 1 or 2 (lanes 1–4). mAb 1H1, raised against peptide A, gave a pattern similar to 2D4 (not shown). The blot used with antibody 2F10 corresponds to a slightly shorter migration of the proteins. On extracts of the full-length construct all mAbs detected an ~30 kDa protein and smaller products, depending on the antibody (the faint larger products seen with 2D4 in lane 2 and with 1G2 in lane 1 are loading artifacts and not endogenous cross-reacting proteins, since they are not seen in the other lanes with the same antibody).

conformational epitopes. In agreement with this hypothesis, mAb 1D4 showed cross-reaction with peptide B, encoded by exon 3 (Fig. 1A), but reacted on Western blot only when exon 4-encoded sequences were also present.

Processed frataxin is decreased or absent in Friedreich ataxia patients

Our strongest reacting antibody, mAb 1G2, was used to detect endogenous frataxin on Western blots of normal human muscle, heart, cerebellum and spinal cord extracts. In all tissues the 1G2 antibody detected an 18 kDa protein corresponding to one of the major smaller products observed in transfected COS-1 cells (Fig. 2). This indicates that frataxin is processed into a smaller mature form by proteolytic cleavage, the larger products presumably representing intermediates of the maturation process. The same, though fainter, band was obtained with mAbs 1D4 (Fig. 2A) and 2F10. mAbs 1H1 and 2D4 failed to detect endogenous frataxin, indicating that the N-terminal epitope they recognize is removed during maturation.

Proof that the 18 kDa protein is indeed frataxin was obtained by analysis of Friedreich ataxia samples. When tested with mAb 1G2, the 18 kDa protein was reduced or absent in skeletal muscle (Fig. 2B) and cerebral and cerebellar cortex (Fig. 2C) of all tested

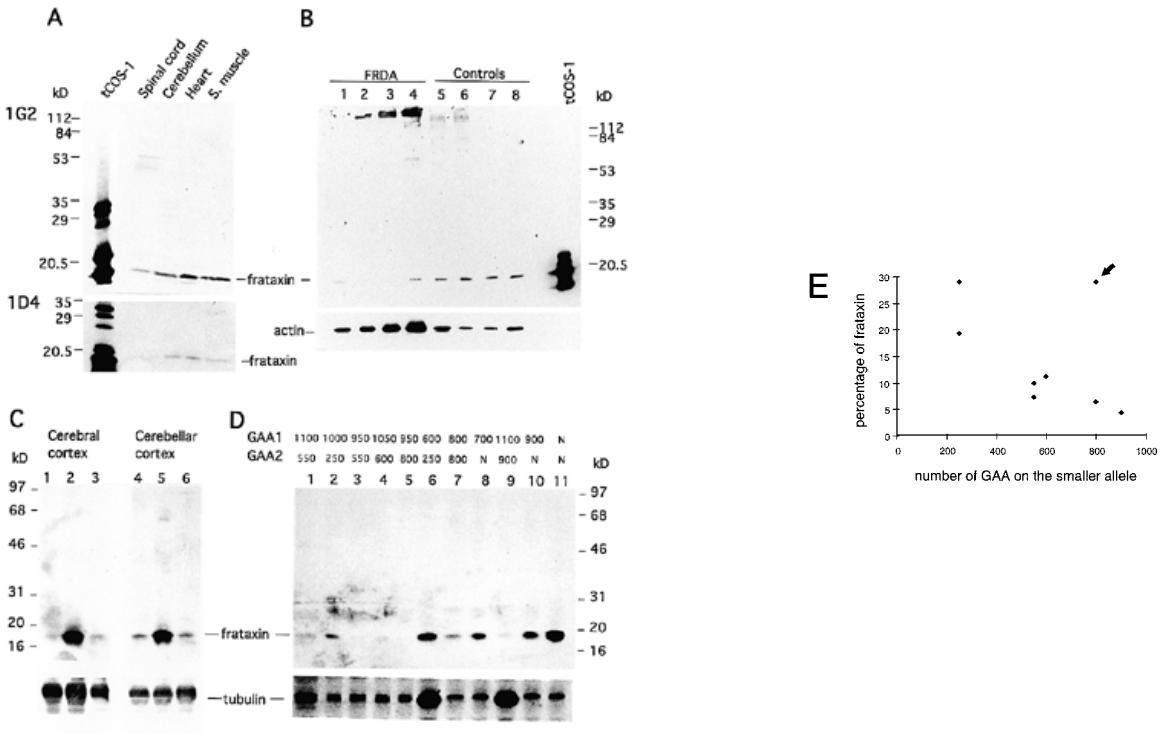

Figure 2. Processed frataxin is decreased in Friedreich ataxia patients. (**A**) Total protein extract (150 µg) from various control human tissues was immunoblotted with mAb 1G2 (top) and 1D4 (bottom). Both mAbs detect an ~18 kDa protein. Cross-reaction with the ~50 kDa protein seen in the spinal cord sample with antibody 1G2 was not reproduced on two other Western blots (not shown). (**B**) Total protein extracts from muscle of Friedreich ataxia patients (FRDA, lanes 1–4) and normal individuals (controls, lanes 5–8) were immunoblotted with mAb 1G2 (top). The same filter was reproved with anti-actin antibody after stripping the anti-frataxin antibody (bottom). The sizes of the smaller expanded alleles of patients 2 and 4 are 570 and 370 GAA respectively. Patient 3 has a 670 GAA expansion and a missense mutation in exon 4 (see Results). A DNA sample was not available from patient 1 but FRDA diagnosis was confirmed by the presence of an expansion in his carrier sister (370 GAA). Cross-reaction of antibody 1G2 with myosin was verified by successive probing with 1G2 and an anti-myosin antibody on a different blot. The 70 kDa protein seen in lane 4 corresponds to a degradation product of myosin. The more extensive processing of frataxin in the transfected COS-1 cells compared with Figures 1B and 2A is due to a longer expression time (66 versus 42 h) after transformation. (**C**) Immunoblots with anti-frataxin mAb 1G2 (top) of extracts from cerebral and cerebellar cortex of Friedreich ataxia patients (lanes 1, 3, 4 and 6) and a normal individual (lanes 2 and 5). (**D**) Immunoblot of lymphoblast cell line extracts from eight FRDA patients (lanes 1–7 and 9), two FRDA carriers (lanes 8 and 10) and a control (lane 11), probed with anti-frataxin antibody (top). Expansion sizes for the patients are indicated above each lane (N, GAA repeats are <50). Blots (C) and (D) were reprobed with anti-tubulin mAb (bottom). Lanes 6 and 9 were overloaded compared with the other lanes, explaining the apparently normal level of frataxin in sample 6 from a patient with a small expansion size (250 GAA). (**E**) Correlation between size of the GAA repeats on the smaller allele and the level of residual frataxin in lymphoblastoid cell lines. The arrow points to the data point corresponding to the 'Acadian' patient.

patients. mAb 1D4 generated a similar result, but also cross-reacted with several unidentified proteins that did not show variation between control and FRDA samples (not shown). Relative loading of total protein extracts was verified by probing the same blots with an antibody directed against a control protein (actin or tubulin). One patient is a compound heterozygote for an expansion mutation $(GAA)_{670}$ and a missense mutation in exon 4 (G130V; M.Cossée, personal communication). This patient has no detectable frataxin in his muscle (Fig. 2B, lane 3). We tested whether the absence of detection could be due to absence of binding by expressing the mutant form in COS-1-transfected cells. Comparison with the 2D4 antibody, directed against the frataxin N-terminus, indicated that 1G2 binding is affected by the missense mutation (not shown), explaining in part the lack of frataxin detection in this patient. This further maps the 1G2 epitope in the first part of the exon 4-encoded sequence.

Correlation between age of onset, disease progression and the expansion mutation suggested that the length of the expansion modulates the amount of residual frataxin present in patients and hence clinical severity (5–9). To test this hypothesis we analysed the amount of residual frataxin in lymphoblastoid cell lines from eight Friedreich ataxia patients with known GAA expansion sizes (Fig. 2D). The residual amount of frataxin varied between 4 and 29% of the level in the normal control. Some inverse correlation was observed between the residual frataxin level and size of the GAA repeat on the smaller allele (GAA1, $r = –0.51$) (Fig. 2E). Inspection of the data showed that in seven patients the residual frataxin level appeared to be strongly dependent on the size of GAA1 ($r = –0.84$, $P = 0.009$), but a single patient (lane 7) had a much higher residual frataxin level than expected from expansion size. While the other seven patients have typical FRDA and evident neurological impairment, this patient is a 12-year-old, almost asymptomatic individual with 'Acadian' FRDA, a milder form of FRDA observed in a specific population with a founder effect (7,14) who came to medical attention only because of a slight pes cavus foot deformity, without any ataxia symptoms. Neurological examination in this case revealed absent reflexes but normal coordination and deep sensation.

Frataxin is a mitochondrial protein

A major clue for unravelling the function of a new protein is to identify its subcellular localization. Immunocytofluorescence with antibody 1G2 revealed granular cytoplasmic staining in transfected COS-1 and HeLa cells overexpressing frataxin (Fig. 3A), as well as in non-transfected cultured mouse astroglial and neuronal cells with only endogenous frataxin expression (Fig. 3B). Staining often appeared elongated and sometimes fibrillar, a typical morphology for mitochondria. To confirm the mitochondrial identity of the frataxin-positive cytoplasmic organelles, double indirect immunocytofluorescence was first performed in transfected HeLa cells. Identical staining was obtained with both mAb 1G2 (red) and an autoimmune anti-mitochondrial antibody (Menarini Diagnostic; green). Co-localization of the two antibodies was demonstrated by the appearance of an intermediate colour (yellow; Fig. 3A). Subcellular localization of frataxin was not altered by overexpression, since identical staining was again obtained in non-transfected mouse astroglial and neuronal cells using mAb 1G2 (red) and MitoTracker Green (Molecular Probes), a mitochondrial-specific fluorescent dye (Fig. 3B). Frataxin staining appeared very strong in the axons of cultured neurons, corresponding to the high number of mitochondria in axons, where high energy consumption takes place.

We obtained independent support for a mitochondrial localization of endogenous frataxin by subcellular fractionation using differential centrifugation. Frataxin was detected weakly in the low speed nuclear pellet fraction (P1), which contains mostly nuclei and cytoskeletal elements. After centrifugation at high speed, the post-mitochondrial supernatant contained almost no detectable frataxin and the twice washed mitochondrial pellet (P2) showed a very clear frataxin enrichment (Fig. 4). Co-purification of frataxin with subunit II of cytochrome c oxidase in the P2 fraction supports the hypothesis that frataxin is a mitochondria-associated protein.

We tested several truncated forms of frataxin in order to localize the mitochondrial target signal. All C-terminally truncated frataxin constructs were located in mitochondria, indicating that the mitochondrial target signal is encoded in exon 1 or 2 (Fig. 5A). N-terminally truncated frataxin that lacks exon 1-encoded sequences presented with a diffuse cytoplasmic and nuclear localization (Fig. 5B) and when both exons 1 and 2 encoded-sequences are missing the truncated protein is not detected at all (not shown). The mitochondrial target signal was further localized by fusing the N-terminal portion of frataxin to a fluorescent tag, green fluorescent protein (GFP). The first 20 amino acids of frataxin were sufficient to target a GFP fusion protein to the mitochondria, as shown by the similar pattern revealed by GFP fluorescence (Fig. 5D) and by the autoimmune anti-mitochondrial antibody (Fig. 5E). Since basic amino acids are important residues in the consensus of the mitochondrial signal peptide (15), we mutated the two arginine residues at positions 6 and 7 into prolines in the full-length frataxin expression vector. The resulting protein, detected with mAb 1G2, appeared to have a diffuse cytoplasmic and nuclear localization (not shown).

Immunocytoelectron microscopy (EM) was performed by peroxidase pre-embedding staining on transfected HeLa cells overexpressing full-length frataxin, due to the low abundance of endogenous frataxin. It was important to permeabilize the cellular membranes with saponin, a mild detergent, in order to allow antibody penetration with minimal damage to cell morphology. Ultrathin sections were analysed by EM with no counterstaining. The labelling was located at the level of the mitochondrial membranes and crests (Fig. 6). The negative control (omission of 1G2 antibody) was devoid of electron-dense deposit. The results indicate that frataxin localizes at or near the inner mitochondrial membrane.

DISCUSSION

The discovery of a large intronic trinucleotide expansion as the cause of an autosomal recessive disease was unexpected and raised the question of the pathogenetic mechanisms involved. Initial experiments, first by semi-quantitative PCR (4) and then by RNase protection (10), indicated that the level of frataxin RNA is severely reduced in patients. These results, and the finding of truncating point mutations in the frataxin gene causing the same clinical presentation (4), suggested a loss of function mechanism, in accordance with the recessive mode of inheritance of the disease. In order to unravel the function disrupted by frataxin mutations and to directly test the steady-state amount of frataxin present in patients, we raised specific monoclonal antibodies. The molecular weight of the full-length frataxin molecule produced from an eukaryotic expression vector appeared larger than predicted (30 versus 23 kDa), suggesting either post-translational modification or aberrant electrophoretic mobility. The identity in size with full-length frataxin produced in an *in vitro* translation assay indicated that frataxin has aberrant electrophoretic mobility. The finding of smaller products in overexpressing COS-1 cells suggested that frataxin is processed. Detection of endogenous frataxin in human tissues confirmed this hypothesis. A single 18 kDa protein is detected with mAbs 1G2, 1D4 and 2F10 and corresponds to the major processed form seen in overexpressing COS-1 cells. The absence of detection of the mature frataxin form with mAbs 1H1 and 2D4 indicates that the N-terminus is removed during processing at least up to the end of exon 1, which accounts for ~6 kDa of the total size decrease.

The severe reduction in the amount of the 18 kDa protein observed in muscle and lymphoblastoid cell lines from FRDA patients proves that it is indeed frataxin and is in full agreement with the previously observed reduction in the frataxin transcript (10). Clinical and molecular studies of a large series of patients demonstrated that the length of the smaller expanded allele accounts for 50% of the variance in age of onset, suggesting that a milder presentation might be the consequence of higher residual frataxin present in the tissues of patients (5–9). We found an inverse correlation between the amount of protein produced in lymphoblastoid cell lines of seven typical FRDA patients and the length of the repeat expansion on the smaller allele. Strong departure from the curve was observed in a single, almost

Figure 3. Transfected and endogenous frataxin co-localize with mitochondria. (**A**) HeLa cells that had been transiently transfected with the frataxin gene were double stained with frataxin mAb 1G2 (red) and anti-mitochondria human serum (green). Green and red signals overlap (yellow pattern), indicating co-localization of frataxin in mitochondria. (**B**) (Left) Immunofluorescence analysis of non-transfected mouse astroglial and neural cells showing that staining of endogenous frataxin (red) is similar to the pattern obtained by staining with MitoTracker (green). (Right) Granular localization of endogenous frataxin in the projections of astroglial cells (centre) and in the axon of a neuron (cell body on the bottom right).

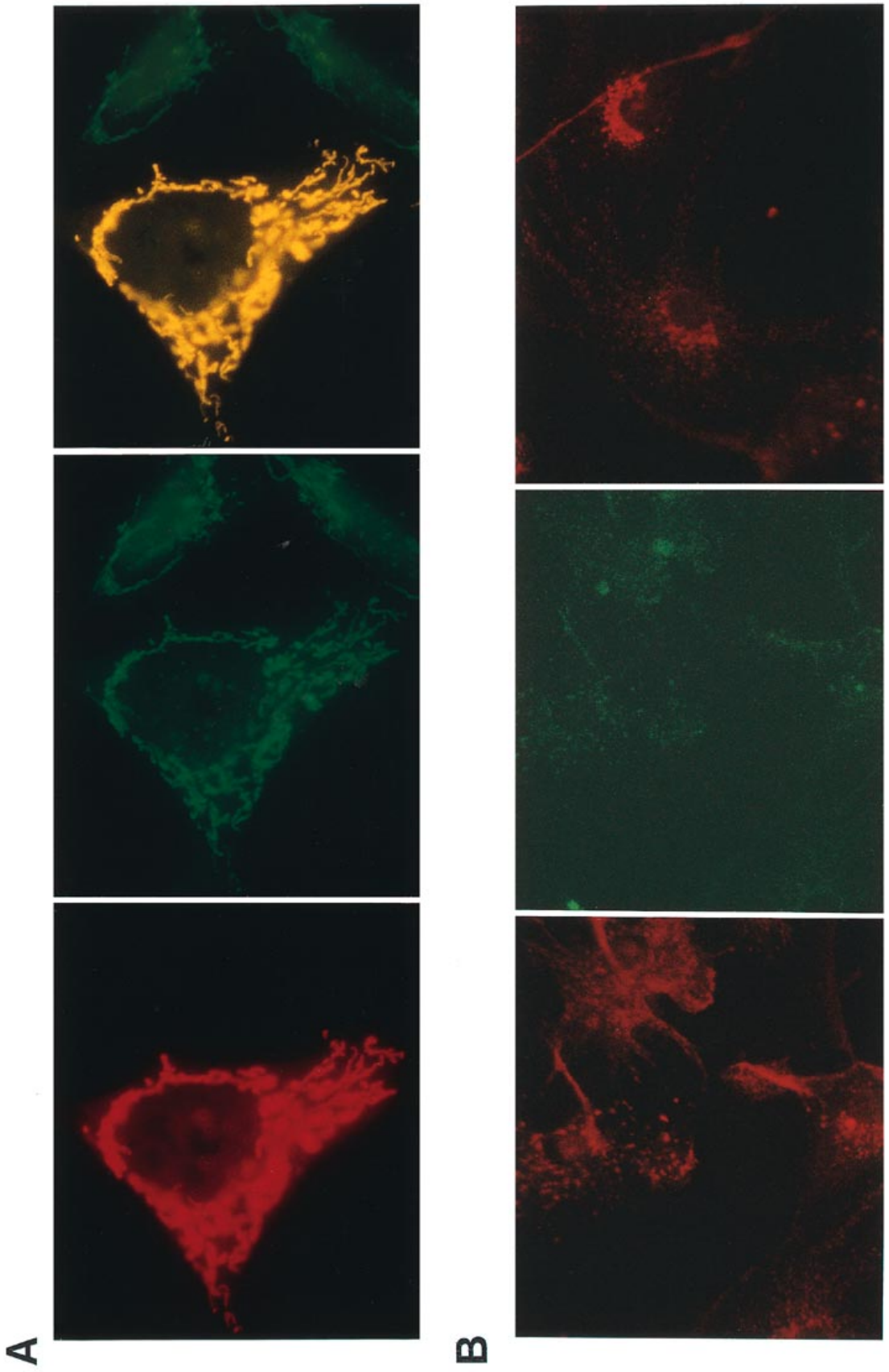
A
B

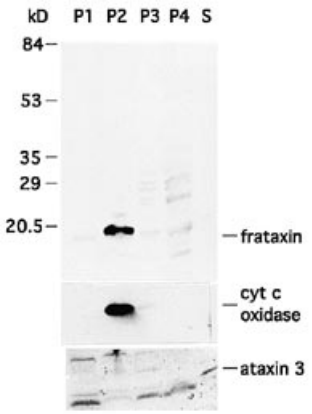

Figure 4. Frataxin is in the same subcellular fraction as cytochrome *c* oxidase. Successive probing of a Western blot of subcellular fractions of a human lymphoblastoid cell line with anti-frataxin 1G2 (top), anti-subunit II of cytochrome *c* oxidase (middle) and anti-ataxin 3 antibodies (bottom). P1, nuclei; P2, plasma membranes and mitochondria; P3, endoplasmic reticulum membranes and peroxisomes; P4, microsomes; S, supernatant. The protein detected immediately below ataxin 3 is a cross-reacting product from the previous antibody, showing the presence of proteins in fractions P1, P3 and P4. Analysis of the same fractions with anti-FMR1 antibodies (35) revealed, as expected, a clear enrichment in the P3 and P4 fractions (not shown).

asymptomatic 'Acadian' patient. Interestingly, FRDA patients of 'Acadian' origin have a significantly milder phenotype which could not be accounted for by differences in expansion size or by differences in the frataxin coding sequence (7). Reduction of frataxin amount appears therefore to represent the molecular basis of the clinical variability in severity and age of onset and is a consequence of the expansion mutation. The finding in the single 'Acadian' patient, if confirmed in additional cases from the same population, suggests, however, the existence of sequence variants resulting in higher expression of the frataxin gene.

A study based on the identification of very rare transcripts suggested that Friedreich ataxia might be due to a defect of hybrid molecules comprising both frataxin and a phosphatidyl-inositol-4-phosphate 5-kinase domain encoded by the neighbouring gene (16). The significance of these rare transcripts in relation to the pathology is highly questionable, particularly in the light of a Friedreich ataxia-causing mutation in the initiating ATG that is not translated in any of the described rare hybrid transcripts (10). We show here that in several tissues there is a single small protein containing frataxin sequences. The results fit well with the presence of a major transcript detected on Northern blots (4). A hybrid molecule containing both frataxin and the phosphatidylinositol-4-phosphate 5-kinase domain would have a larger molecular weight and therefore cannot be the 18 kDa protein absent in Friedreich ataxia patients, seriously challenging the role of phosphatidylinositol-4-phosphate 5-kinase in the pathology of the disease.

We sought to define the subcellular localization of frataxin, as a first step in unraveling its function. Frataxin clearly appears to be localized in mitochondria in both overexpressing, transfected cells and non-transfected astrocytes and neurons, the latter being a cell type that degenerates in FRDA. This subcellular localization clarifies several aspects of frataxin expression and phylogeny. Frataxin is highly expressed in tissues that are rich in mitochondria, such as liver, heart, pancreas and muscle (4), but also in brown fat, thymus and kidney (11). Frataxin is highly conserved throughout evolution (4) and its most distant relative is the CyaY protein of Gram-negative bacteria. The fact that Gram-negative bacteria share a common ancestor with the precursor of eukaryotic mitochondria led Gibson *et al.* (12) to speculate that the frataxin gene might be an ancestral mitochondrial gene that underwent transfer to the nuclear genome during mitochondrial/host cell endosymbiosis. Knock-out of the yeast frataxin counterpart led to a rho$^-$ phenotype with deficiency of mitochondrial respiration (11,17,18). The biochemical defect in patients must certainly be more subtle than in yeast, in order to account for the very slowly progressive nature of the disease, possibly reflecting the presence of residual frataxin. No alteration in mitochondrial DNA of Friedreich ataxia patients has been observed in 10 lymphoblastoid cell lines and two heart samples tested by large fragment PCR (19; A.Rötig, personal communication) and in one heart and three brain samples tested by Southern blot (M.Pandolfo and E.Shoubridge, unpublished results). The mitochondrial localization of frataxin definitively establishes FRDA as a mitochondrial disease caused by loss of function of a nuclear-encoded protein. We also demonstrate that human frataxin contains a functional mitochondrial targeting signal, despite the low match with the mitochondrial targeting sequence consensus. A mitochondrial targeting signal was predicted from analysis of the yeast and mouse frataxin sequences (11). The mitochondrial targeting signal is located within the first 20 amino acids and is cleaved during mitochondrial import and maturation.

Mitochondrial dysfunction has long been suggested for Friedreich ataxia (20) because mitochondria have special relevance for the three most affected tissues in the disease, i.e. neurons, heart and pancreas. However, no consistent metabolic dysfunction had been observed to support a mitochondrial defect in Friedreich ataxia. Mitochondrial enzyme assays have so far been inconclusive, with unconfirmed reports of reduced activity for a few enzymes [for example glutamate dehydrogenase (21), mitochondrial malic enzyme (22), NADH cytochrome *c* reductase, succinate dehydrogenase and succinate cytochrome *c* reductase (23)]. On the other hand, some mitochondrial diseases, such as MERRF (24), NARP (25) and Leigh syndrome (26), share clinical features with FRDA, including ataxia, peripheral neuropathy and cardiomyopathy. Striking clinical similarities between Friedreich ataxia and ataxia with isolated vitamin E deficiency (AVED) (27) may give a clue to frataxin function. AVED is caused by mutations in the α-tocopherol transfer protein (28). Vitamin E is a lipid-soluble antioxidant and free radical scavenger found in cell membranes. It is most abundant in the nuclear and mitochondrial membranes (29). In an *in vitro* assay on rat liver mitochondria, vitamin E, but not superoxide dismutase, was shown to have a protective role against both lipid peroxidation and mitochondrial DNA damage (30). On the other hand, mitochondria are known to be the most important physiological source of superoxide radicals in animal cells (31,32). Strong support in favour of free radical toxicity in Friedreich ataxia comes from studies of the yeast model. Knock-out of the corresponding frataxin gene led to hypersensitivity to hydrogen peroxide and iron (17,18). Iron measurements in the mutant yeast revealed a 10-fold increase in mitochondrial iron, while total iron content was roughly normal. Yeast frataxin was excluded from the mitochondrial outer

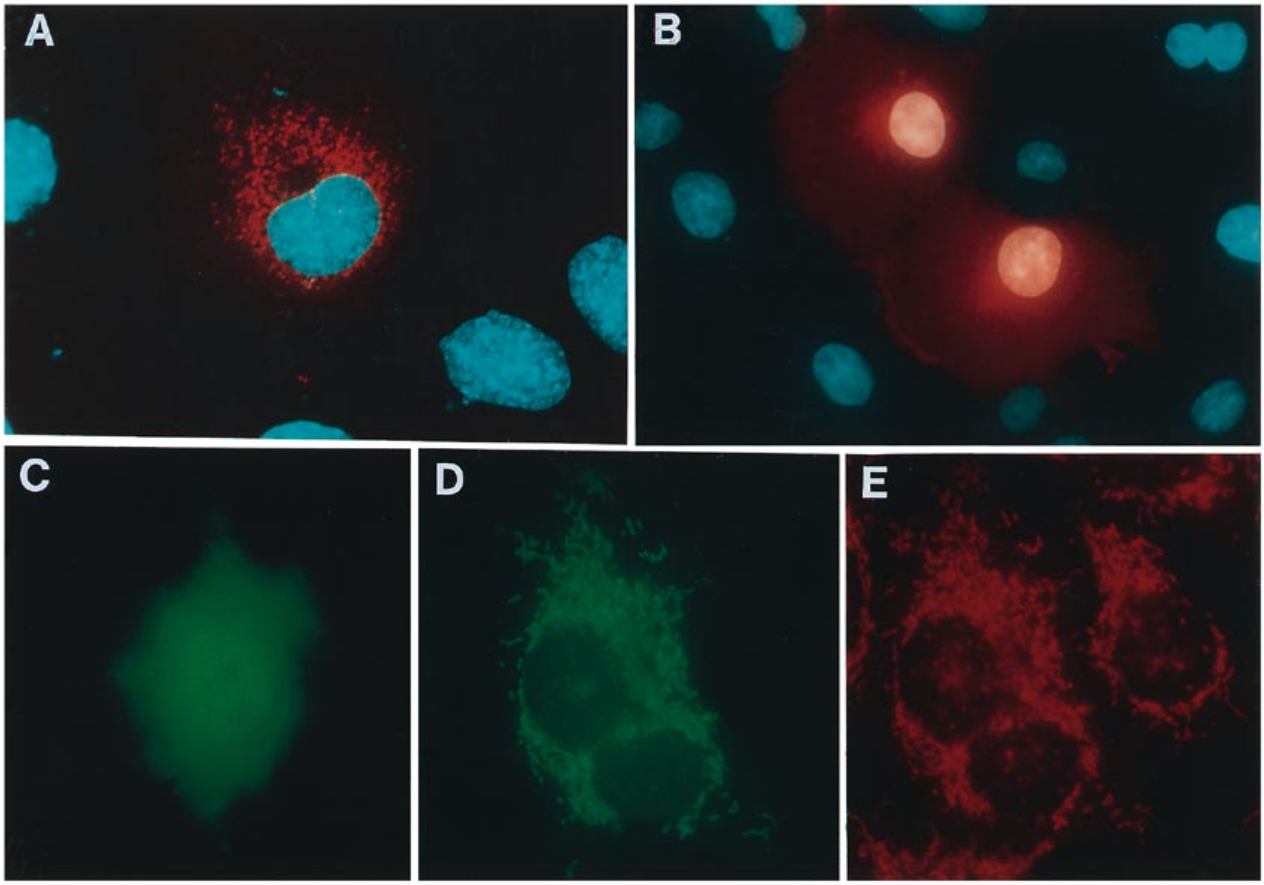

Figure 5. The first 20 amino acids of frataxin are sufficient for mitochondrial targeting. (**A**) Immunofluorescence of a transiently transfected HeLa cell with a construct expressing only exons 1 and 2 of frataxin. The truncated protein was detected using mAb 1H1. (**B**) Detection of an N-terminally truncated frataxin lacking exon 1 with mAb 1G2. In (A) and (B) frataxin stained in red and DNA stained in blue with Hoescht 33258. (**C**) Staining pattern of a transiently transfected HeLa cell with a construct expressing the fluorescent protein GFP alone. (**D**) Expression of the first 20 amino acids of frataxin (MWTLGRRAVAGLLASPSPAQ) fused at the C-terminus with GFP in transiently transfected HeLa cells. The staining matches that with the anti-mitochondria antibody (**E**). The two arginines underlined in the targeting sequence were simultaneously mutated in subsequent experiments (see Results).

membrane (17) and we found human frataxin in the mitochondrial membranes and crests, suggesting that frataxin is located at or near the inner mitochondrial membrane. Frataxin might therefore be involved with iron transport through the membrane or with electron transport by cytochromes and iron sulphur proteins of the mitochondrial inner membrane. Alteration of iron metabolism due to a reduction in frataxin would cause overproduction of free radicals within the mitochondria through the iron-catalysed Fenton chemistry, resulting in a neurodegenerative pathway similar to that seen in isolated vitamin E deficiency. Demonstration that mitochondrial iron metabolism is altered in Friedreich ataxia is needed to confirm that the most frequent hereditary ataxia can be added to the growing list of neurodegenerative diseases caused by free radicals and reactive oxygen species (33,34).

MATERIALS AND METHODS

Construction of expression vectors

The complete coding sequence of frataxin was constructed by PCR amplification of a genomic fragment from positions +1 to +164 and cloning into the *Eco*RI and *Cla*I sites of the frataxin RACE cDNA (4), followed by addition of the *Xba*I–*Hin*dIII 3′ fragment of EST clone 126314 (positions +270 to +1000) (Washington University–Merck EST Project). The PCR 5′ primer contained an artificial *Eco*RI site introduced for cloning purposes. Synthesis of frataxin for immunization was achieved by cloning the entire coding sequence in the *Eco*RI and *Hin*dIII sites of the pATH1 prokaryotic expression vector (13) and production of a TrpE–frataxin fusion protein.

Frataxin was also expressed in eukaryotic cells by cloning the complete coding sequence or different fragments of the frataxin cDNA into the pTL1 expression vector (35). These fragments were generated by PCR with appropriate primers flanked by artificial restriction sites used for cloning. The same strategy was used to construct the GFP expression vectors (pEGFP-C1; Clontech) (36). Mutagenesis of the mitochondrial target sequence and of Gly130 to Val was carried out by PCR with specific primers containing the mutations. The ORF of all constructs (including the PATH1 constructs) was verified by sequencing. COS-1 and HeLa cells were transfected with the plasmids using calcium phosphate precipitation (37). The full-length frataxin

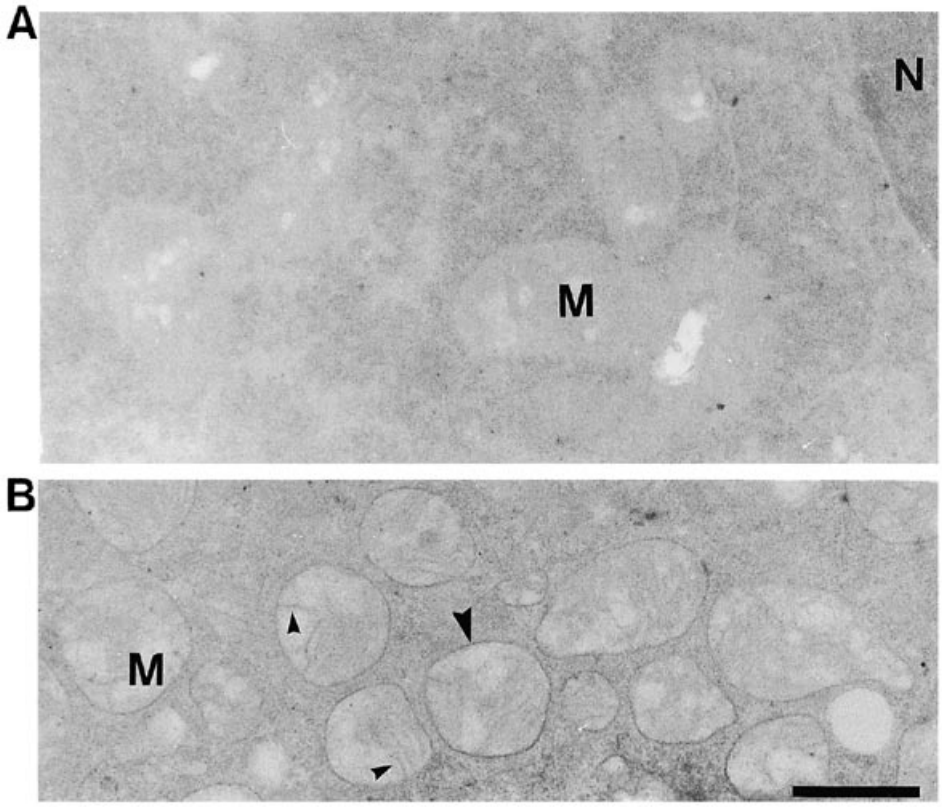

Figure 6. Immunoelectron microscopy reveals that frataxin is associated with mitochondrial membranes in transfected HeLa cells. (**A**) Negative control without primary antibody. (**B**) Pre-embedding mAb 1G2 peroxidase immunodetection labels the mitochondrial external membranes (large arrow heads) and crests (small arrow heads). M, mitochondria; N, nucleus. Scale bar 1 μm.

clone in the pTL1 expression vector was used in an *in vitro* transcription and translation reaction with the TNT system (Promega).

Monoclonal antibody production

Expression of the fusion protein by the pATH vector was induced by growing cells in M9 medium with indolacetic acid and without Trp (13). The fusion protein represented 50–80% of the proteins found in inclusion bodies. Inclusion bodies were solubilized in 8 M urea and proteins were renaturated by sequential dialysis with decreasing concentrations of urea. The synthetic peptide used for immunization (peptide A, CGLRTDIDATCTPRRASSNQRG) was conjugated to ovalbumin (Sigma) (38) prior to injection. Mouse injections and fusions were carried out as described (35). Hybridoma culture supernatants were screened using ELISA tests, immunocytochemistry on COS-1 cells expressing the full-length frataxin and Western blots. Five hybridomas were established and the corresponding antibodies were produced in mice ascites fluids. The weakly reacting antibodies were further purified from ascite fluids by affinity with the TrpE–frataxin fusion protein (39). Class and subclass were determined using an isotyping kit (Amersham). mAbs 1G2, 2D4, 2F10 and 1H1 are all IgG_1,k and mAb 1D4 is a mixture IgG_1,k and IgG_{2a},k.

Western blot analysis

Whole-cell extracts of transfected COS-1 and HeLa cells or of lymphoblastoid cell lines were obtained by homogenization in 50 mM Tris–HCl, pH 8.0, 10% (v/v) glycerol, 5 mM EDTA, 150 mM KCl, 1 mM phenylmethylsulphonyl fluoride followed by sonication. Insoluble material was removed by centrifugation at 10 000 *g* at 4°C for 10 min. Extracts of human tissues were obtained by grinding the frozen biopsies into powder with a pestle and mortar and homogenization in SDS lysis buffer containing 100 mM Tris–HCl, pH 9.0, 2% SDS, 5% β-mercaptoethanol and 15% glycerol. The viscous extracts were heat denatured by boiling for 5 min followed by extensive sonication (2 min) to shear the DNA. Insoluble material was removed by centrifugation and protein concentration was estimated by SDS–PAGE with staining with Coomassie blue. Total protein extracts (50–200 μg) were analysed on 12 or 15% SDS–polyacrylamide gels. Proteins were transferred to nitrocellulose membranes which were blocked with 4% non-fat milk and then incubated with the different primary antibodies, anti-frataxin (ascites fluid diluted 1:5000 or 1:10 000), anti-ataxin 3 (Y.Trottier, unpublished results), anti-actin (Sigma) or anti-subunit II of cytochrome c oxidase (a gift of Dr Anne Lombès) overnight at 4°C. Secondary antibody (goat anti-mouse or anti-rabbit IgG) coupled to peroxidase was used for detection of the reaction with Supersignal Substrate Western blotting

(Pierce, IL) or with the ECL kit (Amersham), according to the manufacturers' instructions. Quantitation of frataxin in lymphoblast immunoblots was obtained by analysing autoradiograms on a video camera image with ISO 9000 software. The intensity of each frataxin band was corrected according to the intensity of the ~50 kDa tubulin band obtained in the same lane after rehybridization of the blot with control anti-tubulin antibodies (Amersham). One homozygous normal individual and two heterozygous carriers, assumed to have 50% frataxin, were used as controls for the amount of frataxin. Measurements were made in triplicate.

Immunocytofluorescence and immunocytoelectron microscopy analysis

Differentiated striatal neurons and glia were generated from normal mouse E14 striatal CNS stem cell cultures isolated from embryonic CD1 albino mice, as described elsewhere (40). Briefly, following mechanical dissociation E14 single striatal cells were plated at a final density of 50 000 cells/cm^2 in SATO/N2 basal medium in the presence of 20 ng/ml epidermal growth factor (EGF). Proliferating cultures were serially passaged every 6 days, three times, by mechanical dissociation and replating into the same EGF-containing medium. Six days after the last subculturing single clones (spheres) of cells were plated onto Matrigel (Becton Dickinson, Sparks, MD)-coated glass coverslips and grown in the presence of EGF for an additional 2 days after plating. Differentiation was then triggered by EGF removal and the cells were allowed to differentiate in EGF-free basal medium (control) for an additional 5 days. Viable cultures were exposed for 40 min at 37°C to 200 nM MitoTracker Green FM (containing a thiol-reactive chloromethyl moiety; Molecular Probes, Eugene, Oregon) diluted in control medium. Coverslips were rinsed once with control medium and once with phosphate-buffered saline (PBS), pH 7,4 prior to fixation for 15 min with 4% paraformaldehyde in PBS. After rinsing with PBS, coverslips were incubated for 10 min at room temperature in cold acetone followed by double washings with PBS, 10% NGS. Samples were then incubated for 1 h at 37°C with the primary anti-frataxin monoclonal antibody 1G2, diluted 1:100 in PBS, 10% NGS. After thorough washing with PBS, 10% NGS cells were reacted for 45 min at room temperature with secondary rhodamine (TRITC)-conjugated goat anti-mouse antibody (1:100; Boehringer Mannheim, Indianapolis, IN), rinsed three times in PBS and mounted on glass slides with Fluorsave (Calbiochem, La Jolla, CA). No labelling was ever observed in control experiments in which primary antibody and/or MitoTracker were omitted and neither was there evidence of cross-reactivity between MitoTracker and the secondary rhodamine (TRITC)-conjugated goat anti-mouse antibody.

Transfected HeLa cells, growing in Leighton tubes, were washed in PBS, fixed in 4% paraformaldehyde (20 min) and permeabilized in 0.05% Triton X-100 (3 × 5 min). Cells were then incubated for 16 h at 4°C with mAb 1G2 (ascites fluid 1:1000). Specifically bound antibodies were directly revealed by Cy3-conjugated goat anti-mouse antibody (Jackson Immunoresearch Laboratories). In co-localization experiments a second human autoimmune anti-mitochondrial primary antibody (Menarini diagnostics) was added and revealed with a FITC- or Texas red-conjugated anti-human antibody (Jackson Immunoresearch Laboratories).

For electron microscopy studies transfected cells growing in Leighton tubes were fixed for 5 h at 4°C with 4% paraformaldehyde, 0.1% glutaraldehyde, in 0.1 M phosphate buffer, pH 7.3, and then incubated for 16 h at 4°C with antibody 1G2 (1:1000) in the presence of 0.1% saponin. The primary antibody was revealed using the ABC method (Vector Laboratories Inc., CA) and diaminobenzidine as peroxidase substrate. Transfected cells were first detected at the optical level, then processed for standard EM methods, sliced in ultrathin 70 nm sections and transferred to electron microscopy grids. Control experiments, where the primary antibody was omitted, were performed in parallel.

Subcellular fractionation of lymphoblastoid cells

The method of Lee *et al.* (41) was used to separate nuclei and cytoplasm. The cytoplasmic supernatant was further fractionated according to standard differential centrifugation methods. Protein concentration was determined by Bradford assay (42) and 100 µg total protein were loaded per lane.

ACKNOWLEDGEMENTS

We wish to thank Dr A.Lombès for the anti-cytochrome *c* oxidase antibody, Dr R.Gatti for lymphoblastoid cell lines and Drs T.Gibson and F.Foury for sharing unpublished results. Thanks are due to Dr Cossée for analysis of patients and discussions and to H.Koutnikova for discussions. We are grateful to L.Reutenauer, S.Vicaire, F.Ruffenach, N.Jung, F.Cottin and V.Schultz for their technical assistance. This work was supported by funds from the Association Française contre les Myopathies (AFM), CNRS, INSERM and the Ministère de l'Enseignement Supérieur et de la Recherche (M.K.) and by grants from the National Institutes of Health (NS34192) and the Muscular Dystrophy Association, USA (M.P.). V.C. is the recipient of a fellowship from the EEC and L.M. is the recipient of a fellowship from the Medical Research Council of Canada. Y.T. is the recipient of a fellowship from the Hereditary Disease Foundation (USA).

REFERENCES

1. Harding,A.E. (1983) Classification of the hereditary ataxias and paraplegias. *Lancet*, **i**, 1151–1155.
2. Oppenheimer,D.R. and Esiri,M.M. (1992) In Adams,J.H.,Corselli,J.A.N. and Duchen,L.W. (eds), *Greenfield's Neuropathology.* Edward Arnold, London, pp. 1015–1018.
3. Wallace,D.C., Shoffner,J.M., Trounce,I., Brown,M.D., Ballinger,S.W., Corral-Debrinski,M., Horton,T., Jun,A.S. and Lott,M.T. (1995) Mitochondrial DNA mutations in human degenerative diseases and aging. *Biochim. Biophys. Acta*, **1271**, 141–151.
4. Campuzano,V., Montermini,L., Moltó,M.D., Pianese,L., Cossée,M., Cavalcanti,F., Monros,E., Rodius,F., Duclos,F., Monticelli,A., Zara,F., Cañizares,J., Koutnikova,H., Bidichandani,S., Gellera,C., Brice,A., Trouillas,P., De Michele,G., Filla,A., de Frutos,R., Palau,F., Patel,P.I., Di Donato,S., Mandel,J.-L., Cocozza,S., Koenig,M. and Pandolfo,M. (1996) Friedreich ataxia: autosomal recessive disease caused by an intronic GAA triplet repeat expansion. *Science*, **271**, 1423–1427.
5. Filla,A., De Michele,G., Cavalcanti,F., Pianese,L., Monticelli,A., Campanella,G. and Cocozza,S. (1996) The relationship between trinucleotide (GAA) repeat length and clinical features in Friedreich ataxia. *Am. J. Hum. Genet.*, **59**, 554–560.
6. Dürr,A., Cossée,M., Agid,Y., Campuzano,V., Mignard,C., Penet,C., Mandel,J.-L., Brice,A. and Koenig,M. (1996) Clinical and genetic abnormalities in patients with Friedreich's ataxia. *New Engl. J. Med.*, **335**, 1169–1175.

7. Montermini,L., Richter,A., Morgan,K., Justice,C.M., Julien,D., Castelloti,B., Mercier,J., Poirier,J., Capazzoli,F., Bouchard,J.P., Lemieux,B., Mathieu,J., Vanasse,M., Seni,M.H., Graham,G., Andermann,F., Andermann,E., Melançon,S., Keats,B.J.B., Di Donato,S. and Pandolfo,M. (1997) Phenotypic variability in Friedreich ataxia: role of the associated GAA triplet repeat expansion. *Annls Neurol*., **41**, 675–682.
8. Lamont,PJ., Davis,MB. and Wood,NW. (1997) Identification and sizing of the GAA trinucleotide repeat expansion of Friedreich's ataxia in 56 patients. Clinical and genetic correlates. *Brain*, **120**, 673–680.
9. Monros,E., Moltó,M.D., Martinez,F., Cañizares,J., Blanca,J., Vilchez,J.J., Prieto,F., de Frutos,R. and Palau,F. (1997) Phenotype correlation and intergenerational dynamics of the Friedreich ataxia GAA trinucleotide repeat. *Am. J. Hum. Genet*., **61**, 101–110.
10. Cossée,M., Campuzano,V., Koutnikova,H., Fischbeck,K.H., Mandel,J.-L., Koenig,M., Bidichandani,S., Patel,P.I., Moltó,M.D., Cañizares,J., de Frutos,R., Pianese,L., Cavalcanti,F., Monticelli,A., Cocozza,S., Montermini,L. and Pandolfo,M. (1997) Frataxin fracas. *Nature Genet*., **15**, 337–338.
11. Koutnikova,H., Campuzano,V., Foury,F., Dollé,P., Cazzalini,O. and Koenig,M. (1997) Studies of human, mouse and yeast homologues indicate a mitochondrial function for frataxin. *Nature Genet*., **16**, 345–351.
12. Gibson,T.J., Koonin,E.V., Musco,G., Pastore,A. and Bork,P. (1996) Friedreich's ataxia protein: bacterial homologs point to mitochondrial dysfunction. *Trends Neurosci*., **19**, 465–468.
13. Dieckmann,C.L. and Tzagoloff,A. (1985) Assembly of the mitochondrial membrane system. CBP6, a yeast nuclear gene necessary for synthesis of cytochrome b. *J. Biol. Chem*., **260**, 1513–1520.
14. Barbeau,A., Roy,M., Sadibelouiz,M. and Wilensky,M.A. (1984) Recessive ataxia in Acadians and 'Cajuns'. *Can. J. Neurol. Sci*., **11**, 526–533.
15. Schatz,G. and Dobberstein,B. (1996) Common principles of protein translocation across membranes. *Science*, **271**, 1519–1526.
16. Carvajal,J., Pook,M.A., dos Santos,M., Doudney,K., Hillermann,R., Minogue,S., Williamson,R., Hsuan,J.J. and Chamberlain,S. (1996) The Friedreich's ataxia gene encodes a novel phophatidylinositol-4-phosphate 5-kinase. *Nature Genet*., **14**, 157–162.
17. Babcock,M., de Silva,D., Oaks,R., Davis-Kaplan,S., Jiralerspong,S., Montermini,L., Pandolfo,M. and Kaplan,J. (1997) Regulation of mitochondrial iron accumulation by Yfh1, a putative homolog of frataxin. *Science*, **276**, 1709–1712.
18. Foury,F. and Cazzalini,O. (1997) Deletion of the yeast homologue of the human gene associated with Friedeich's ataxia elicits iron accumulation in mitochondria. *FEBS Lett*., in press.
19. Paul,R., Santucci,S., Saunieres,A., Desnuelle,C. and Paquis-Flucklinger,V. (1996) Rapid mapping of mitochondrial DNA deletions by large-fragment PCR. *Trends Genet*., **12**, 131–132.
20. Cedarbaum,J.M. and Blass,J.P. (1986) Mitochondrial dysfunction and spinocerebellar degenerations. *Neurochem. Pathol*., **4**, 43–63.
21. Barbeau,A., Charbonneau,M. and Cloutier,T. (1980) Leucocyte glutamate dehydrogenase in various hereditary ataxias. *Can. J. Neurol. Sci*., **7**, 421–424.
22. Stumpf,D.A., Parks,J.K., Eguren,L.A. and Haas,R. (1982) Friedreich ataxia: III. Mitochondrial malic enzyme deficiency. *Neurology*, **32**, 221–227.
23. Schöls,L., Reichmann,H., Amoiridis,G., Seibel,P., Wagener,S., Seufert,S. and Przuntek,H. (1996) Mitochondrial disorders in degenerative ataxias. *Eur. J. Neurol*., **3**, 55–60.
24. Fukuhara,N., Tokiguchi,S., Shirakawa,K. and Tsubaki,T. (1980) Myoclonus epilepsy associated with ragged-red fibres (mitochondrial abnormalities): disease entity or a syndrome? Light- and electron-microscopic studies of two cases and review of literature. *J. Neurol. Sci*., **47**, 117–133.
25. Holt,I.J., Harding,A.E., Petty,R.K.H. and Morgan-Hughes,A. (1990) A new mitochondrial disease associated with mitochondrial DNA heteroplasmy. *Am. J. Hum. Genet*., **46**, 428–433.
26. Pastores,G.M., Santorelli,F.M., Shanske,S., Gelb,B.D., Fyfe,B., Wolfe,D. and Willner,J.P. (1994) Leigh syndrome and hypertrophic cardiomyopathy in an infant with a mitochondrial DNA point mutation (T8993G). *Am. J. Med. Genet*., **50**, 265–271.
27. Ben Hamida,M., Belal,S., Sirugo,G., Ben Hamida,C., Panayides,K., Ioannou,P., Beckmann,J., Mandel,J-L., Hentati,F., Koenig,M. and Middleton,L. (1993) Friedreich's ataxia phenotype not linked to chromosome 9 and associated with selective autosomal recessive vitamin E deficiency in two inbred Tunisian families. *Neurology*, **43**, 2179–2183.
28. Ouahchi,K., Arita,M., Kayden,H.J., Hentati,F., Ben Hamida,M., Sokol,R., Arai,H., Inoue,K., Mandel,J.-L. and Koenig,M. (1995) Ataxia with isolated vitamin E deficiency is caused by mutations in the α-tocopherol transfer protein. *Nature Genet*., **9**, 141–145.
29. Guarnieri,C., Flamigni,F. and Caldarera,C.R. (1980) Subcellular localization of alpha-tocopherol and its effect on RNA synthesis in perfused rabbit heart. *Ital. J. Biochem*., **29**, 176–184.
30. Hruszkewycz,A.M. (1988) Evidence for mitochondrial DNA damage by lipid peroxidation. *Biochem. Biophys. Res. Commun*., **153**, 191–197.
31. Naqui,A. and Chance,B. (1987) Steady-state kinetic approaches to complex biological systems. *Cell Biophys*., **11**, 159–176.
32. Nohl,H. and Jordan,W. (1986) The mitochondrial site of superoxide formation. *Biochem. Biophys. Res. Commun*., **138**, 533–539.
33. Gotz,M.E., Kunig,G., Riederer,P. and Youdim,M.B. (1994) Oxidative stress: free radical production in neural degeneration. *Pharmacol. Ther*., **63**, 37–122.
34. Beal,M.F. (1995) Metabolic disorders and neurotoxicology [editorial]. *Curr. Opin. Neurol*., **8**, 467–468.
35. Devys,D., Lutz,Y., Rouyer,N., Bellocq,J.P. and Mandel,J.L. (1993) The FMR-1 protein is cytoplasmic, most abundant in neurons and appears normal in carriers of a fragile X premutation. *Nature Genet*., **4**, 335–340.
36. Gerdes,H.H. and Kaether,C. (1996) Green fluorescent protein: applications in cell biology. *FEBS Lett*., **389**, 44–47.
37. Gorman,C.M., Lane,D.P. and Rigby,P.W. (1984) High efficiency gene transfer into mammalian cells. *Phil. Trans. R. Soc. Lond. (Biol.)*, **307**, 343–346.
38. Harlow,E. and Lane,D. (1988) *Antibodies: A Laboratory Manual*. Cold Spring Harbor Laboratory Press, Cold Spring Harbor, NY.
39. Hoffman,E.P., Brown,R.H.,Jr and Kunkel,L.M. (1987) Dystrophin: the protein product of the Duchenne muscular dystrophy locus. *Cell*, **51**, 919–928.
40. Vescovi,A.L., Reynolds,B.A., Fraser,D.D. and Weiss,S. (1993) bFGF regulates the proliferative fate of unipotent (neuronal) and bipotent (neuronal/astroglial) EGF-generated CNS progenitor cells. *Neuron*, **11**, 951–966.
41. Lee,K.A., Bindereif,A. and Green,M.R. (1988) A small-scale procedure for preparation of nuclear extracts that support efficient transcription and pre-mRNA splicing. *Gene Anal. Techniques*, **5**, 22–31.
42. Bradford,M.M. (1976) A rapid sensitive method for the quantitation of microgram quantities of protein utilizing the principle of protein–dye binding. *Anal. Biochem*, **72**, 248–254.